

Running title: Prognostic Role for SPOP, DAXX, RARRES1, and LAMP2 Genes in Prostate Cancer

Potential Prognostic Role for SPOP, DAXX, RARRES1, and LAMP2 as an Autophagy Related Genes in Prostate Cancer

Leila Jamali¹, Afshin Moradi^{2,3}, Maziar Ganji¹, Mohsen Ayati⁴, Behrang Kazeminezhad⁵, Zahra Fazeli Attar¹, Hamid Ghaedi¹, Seyyed Mohammad Hossein Ghaderian^{1,6*}, Morteza Fallah-Karkan^{7,8}, Arash Ranjbar⁷

¹ Department of Medical Genetics, School of Medicine, Shahid Beheshti University of Medical Sciences, Tehran, Iran.

² Cancer Research Center, Shohada-e-Tajrish Hospital, Faculty of Medicine, Shahid Beheshti University of Medical Sciences, Tehran, Iran.

³ Infertility and Reproductive Health Research Center, Shohada-e-Tajrish Hospital, Faculty of Medicine, Shahid Beheshti University of Medical Sciences, Tehran, Iran.

⁴ Uro-oncology Research Center, Tehran University of Medical Sciences, Tehran, Iran.

⁵ Department of pathology, Shahid Beheshti University of Medical Sciences, Tehran, Iran.

⁶ Urogenital Stem Cell Research Center, Shahid Beheshti University of Medical Sciences, Tehran, Iran.

⁷ Urology resident, Shohada-e-Tajrish hospital, Shahid Beheshti Medical University, Tehran, Iran.

⁸ Laser Application in Medical Science Research Center, Shohada-e-Tajrish Hospital, Faculty of Medicine, Shahid Beheshti University of Medical Sciences, Tehran, Iran.

Keywords: Prostate cancer, Autophagy, Gene Regulatory Network, SPOP, DAXX, RARRES1, LAMP2

Abstract

Purpose: Autophagy plays a critical role in PCa development. *DAXX* has a potent pro-survival effect by enhancing cell growth in PCa via suppression of autophagy. Here, we depicted a network governed by *DAXX* and *SPOP* by which the autophagy pathway is suppressed through the ubiquitination and modulation of key cellular signaling pathways mediators including *LAMP2* and *RARRES1*.

Materials and Methods: Through network-based bioinformatics approaches, the expression levels of *DAXX*, *RARRES1*, *LAMP2*, and *SPOP* genes was assessed in 50 PCa tissues and 50 normal adjacent from the same sample as well as 50 benign prostatic hyperplasia (BPH) tissues by quantitative RT-PCR. The normal adjacent tissues were taken from regions more than 5mm away from the bulk of those tumor tissues with clearly distinct margins. RNA extraction, cDNA synthesis and Real-time Quantitative RT-PCR were done for assessment of gene expression. To evaluate the primary gene network centered on autophagy pathway, according to the Query-dependent weighting algorithm, these two networks were integrated with Cytoscape 3.4 software.

Results: We found that in PCa tissues the *DAXX* expression level was significantly increased ($P < 0.001$) and the expressions of *SPOP*, *RARRES1*, and *LAMP2* were significantly down-regulated, when compared to both control groups including normal adjacent and BPH tissues. Moreover, significant correlations were observed between expression levels of all four genes. Additionally, ROC curve analysis revealed that *LAMP2* had the most sensitivity and specificity.

Conclusion: These findings suggest that the contribution of *SPOP*, *DAXX*, *RARRES1*, and *LAMP2* together could be a putative regulatory element acting as a prognostic signature and therapeutic target in PCa.

Introduction

Prostate cancer (PCa) is the most common malignancy in men⁽¹⁻⁵⁾. Currently, clinicopathological features including Gleason score (GS), staging, and prostate-specific antigen (PSA) are

conventional prognostic markers ^(6,7) and utilized for clinical decision making. Nonetheless, they are insufficiently accurate to discriminate the indolent tumors from aggressive ones due to heterogeneous genetic background of PCa ⁽⁸⁻¹⁰⁾, which emphasizes the inevitable necessity of identifying novel molecular biomarkers and high-risk individuals ⁽¹¹⁻¹³⁾.

Autophagy is a survival-promoting pathway that plays the key role of eliminating damaged cellular compartments and aggregated proteins in lysosomes ⁽¹⁴⁾. Autophagy also can serve as a tumor suppressor via preventing the damaged proteins accumulation. Despite various attempts, role of autophagy and its precise function in PCa, remains unclear ⁽¹⁵⁾.

Various studies have indicated the crucial roles of *speckle-type POZ protein (SPOP)* and *death-domain associated protein (DAXX)* in cell apoptosis, proliferation and that their dysregulated expression may contribute to autophagy pathways in tumorigenesis ^(16,17). Extensive genomic documents have considered *SPOP* as a tumor suppressive role via degradation of oncogenic substrates in malignant prostate cells ⁽¹⁸⁾. *DAXX*, as a transcriptional repressor, in co-operation with other transcription elements participates in regulating *DAPK1/3* tumor suppressor protein kinases ⁽¹⁹⁾, which are associated with autophagy ^(20,21).

As another element relevant to autophagy, *retinoic acid receptor responder 1 (RARRES1)* is a new retinoic inducible gene. Expression of *RARRES1* is known to activate the autophagy pathways. Furthermore, dysregulation in *RARRES1* was indicated to associate with malignant transformations and tumor progression ^(1,22).

Retinoic acid receptors (RARs) signaling controls the activation of *lysosome-associated membrane glycoprotein 2 (LAMP2)* ⁽²³⁾. *LAMP2* encodes a single-span lysosomal membrane protein that is involved in the lysosomal stability. Nonetheless, apart from preserving the structural integrity of lysosomal membranes, a critical role has been proposed for *LAMP2* in lysosomal function and autophagy in the context of cancer ⁽²⁴⁾.

In this study, first we aimed to construct a network for candidate genes participating in autophagy pathway based on literatures to clarify the role of these candidate genes in relation with diverse interactions in cellular networks. We hypothesized these interactions may potentially affect the individual behavioral of each target gene in a context-dependent manner.

Altogether, here we aim to develop network enrichment for *SPOP*, *DAXX*, *RARRES1*, and *LAMP2* genes and to examine their expression levels in PCa tissues in comparison to normal adjacent and BPH tissues.

Materials and methods

Patients and tissue samples

After institutional ethical committee approval (ethics code:IR.SBMU.MSP.REC.1396.286), this case-control study was conducted on a series of 189 paraffin-embedded prostate tissue samples. The exclusion criteria included the blocks with poor histopathological quality, patients who had history of chemoradiotherapy before surgery, presence of other malignancies in patients, and samples with technical problems in tissue processing. Subjects aged from 55 to 79 years in PCa and 59 to 79 years in Benign Prostatic Hyperplasia (BPH) included in study. Finally leaving a total of 150 samples for the final analysis. Our collection included 50 PCa and 50 normal adjacent tissues from the same sample in addition to 50 BPH tissues. Considering the fact that although normal adjacent tissue is normal based on pathological feature, it is abnormal pertaining to molecular changes and there is a potential of tumor progression to adjacent tissue cells over time, so we utilized BPH as secondary external controls. The adjacent normal tissues were taken from regions more than 5 mm away from the bulk of those tumor tissues with clearly distinct margins. One-mm tissue cores were obtained from all samples after processing and were transferred to the RNase-free microtubes for RNA extraction. All samples were diagnosed by an expert pathologist to determine and confirm the differentiation status of adenocarcinoma tissue and dysplasia degree of the adenoma tissues. Evaluation of tumor differentiation was based on the architectural and glandular differentiation as well as tumor nuclear features. Tumor grade was figured out based on GS system according to the 2014 International Society of Urological Pathology (ISUP) Consensus on Gleason Scoring of Prostatic Carcinoma ⁽²⁵⁾. Other parameters such as PT category, prostatic intraepithelial neoplasia (PIN), perineural invasion, and serum PSA levels were included too.

All these samples were gathered from February 2014 to October 2016 from Mehr and Shohada-e-Tajrish Hospitals, Tehran, Iran. The study protocol was approved by the Institutional Review Board of Shahid Beheshti University of Medical Sciences.

Bioinformatic analysis

We designed a network for candidate genes, gathered from literature review, and their cellular interactions with other genes in various signaling pathways were created. The gene Regulatory network drawing was accomplished by STRING 1.1 software with confidence cutoff value of 0.1 for the interactions. As the next step, another gene network was plotted with GeneMANIA prediction server by applying unregularized algorithm. To evaluate the primary gene network centered on autophagy pathway, according to the Query-dependent weighting algorithm, these two networks were integrated with Cytoscape 3.4 software, validated Regulatory Interactions Network Analysis software⁽²⁶⁻²⁸⁾. We applied the Reactome FI 5.2 package to analyze and enrich the gene network and interactions.

RNA extraction and cDNA synthesis

Total RNA extraction was carried out from all samples using Formalin-fixed, paraffin-embedded (FFPE) RNA Purification Kit (Cat. 25300; NORGENE, Canada) according to the manufacture's protocol. The standard de-crosslinking and column purification as well as DNase I treatment were performed to remove proteins and other cellular components in addition to genomic DNA prior to cDNA synthesis. The RNA quality and quantity were measured using agarose gel electrophoresis and Nanodrop 2000 (Thermo Fisher Scientific, Wilmington, DE, USA), respectively. Samples with sufficient yield (>100 ng) and A260/A280 ratio between 1.8–2 were used for single-strand cDNA synthesis. Briefly, 500 ng of total RNA from each sample was subjected to reverse transcription for target gene. cDNA was synthesized utilizing Prime Script II reverse transcriptase (TaKaRa, Japan) by the following method: at 37 °C for 15 minutes (reverse transcription) followed by 85 °C 5 second (inactivation of reverse transcriptase with heat treatment).

Real-time Quantitative RT-PCR (qRT-PCR)

The cDNA was diluted 1:10 in nuclease-free water. Real-time PCR was performed in duplicate in a LightCycler96 instrument (Roche Diagnostics). SYBR Premix Ex Taq II (TaKaRa, Japan) was used for detection of gene expressions. The SYBR qRT-PCR was: 30 sec incubation at 95 °C followed by 40, two step cycles of amplifications consists of 95 °C for 15 sec and 60°C for one min. The formation of PCR products was confirmed through melting curves. Primer sequences were designed by Allele ID software version 7.0 for Windows (Premier Biosoft International, Palo Alto, CA, USA). Exon-exon junction method and NCBI Primer Blast were applied (**Table 1**).

Table 1. The sequences of primers used in this study.

Each run had a negative control (without cDNA template) to check any possible contamination. The relative quantification of expression changes was calculated after normalization to Beta 2Microglobuline (B2M) expression according to previous study⁽²⁹⁾. Data were evaluated using the comparative cycle threshold (CT).

Statistical analysis

Relative quantification of mRNA expression was evaluated using the comparative cycle threshold (CT) method. The expression of samples was normalized to the expression of B2M and fold change was calculated, using the $2^{-\Delta\Delta Ct}$ method.

All statistical analyses were conducted on SPSS statistical software version 20 (SPSS Inc., Chicago IL, USA). Pvalues < 0.05 were considered statistically significant. Mean normalized gene expression \pm SD was calculated from independent experiments. For comparisons between PCa and normal adjacent tissues the normality of the response variables was checked using Shapiro-Wilk statistical test. If normality is accepted, the t test is used; otherwise the Mann-Whitney test or Wilcoxon was utilized for independent non-parametric and dependent variables, respectively. Furthermore, to investigate the correlations, given the normality test of the data the Pearson correlation coefficient for parametric values and Spearman's rank for nonparametric data utilized. Also, to evaluate statistically significant differences between two or more groups of an independent variable one-way ANOVA and Kruskal-Wallis test was used respectively, for parametric and nonparametric data.

In addition, authors represented the receiver operating characteristic (ROC) curve to determine the sensitivity and specificity of gene expression levels as diagnostic markers for PCa. ROC was calculated to determine the potential of genes to discriminate between malignant and non-malignant samples.

Ethics

The ethical committee of Shohada-e-Tajrish Hospital approved this study and permitted us to review patients' medical data. The personal data of the subjects were not disclosed and the principles of patient secrecy were observed.

Results

Clinicopathological characteristics

The mean age and PSA level were 65.49 ± 6.28 years and 10.34 ± 11.10 ng/mL in cancerous sample. The subjects with BPH also had the mean age of 66.35 ± 4.55 with 4.34 ± 1.09 ng/mL PSA level. **Table 2** illustrates the associations between gene expression levels and clinicopathological characteristics, no significant association was found.

Table 2. The association of four candidate genes with clinicopathological characteristics gathered from PCa patients.

Bioinformatic network analysis

The results from network enrichment of STRING and GeneMANIA softwares in terms of statistical significance (False Discovery Rate < 0.25) revealed the interaction of candidate genes with other genes in relation to biological and molecular pathways. During functional categorization analysis, four main modules were identified in gene network, each with up to 11 genes (**Figure 1**). First module included “Co-regulation of androgen receptor (AR) activity” [$P = 1.27E-05$] and “Pathways in cancer” [$P = 3.20E-03$] (comprising *SPOP*, *AR*, *GLI3*, *RNF4*, *PDX1*, *GLI2*, *SHE*, *TMF1*, *SNURF*, *ATRX*, *CUL3* genes). The module of “Class I PI3K signaling” [$P = 4.33E-04$] and “Apoptosis” [$P = 6.53E-03$] (including *DAXX*, *MAP3K5*, *HIPK1*, *UBE21*, *ETS1*, *SLC2A4*, *KDM1A*, *HSPB1*, *RASSF1*, *KIF5B* genes) was also demonstrated in this network. Moreover, the modules of “Lysosome” [$P = 5.92E-03$] and “Phagosome” [$P = 3.87E-03$] (including *RARRES1*, *LAMP2*, *IMPDH1*, *LXN*) as well as “Retinoic acid receptors-mediated signaling” [$P = 1.18E-07$] and “RNA polymerase II transcription” [$P = 1.40E-08$] (comprising genes such as of *ESR1*, *PPARG*, *NR3C1*, *KLK3*, *NCOA2*, *NCOA1*, *RXRA*, *PPARA*, *RARA*) were implicated in this network. The genes in the modules were mainly located in the nucleus, cytoplasm, and lysosome.

Figure 1. The network clustering modules found in this study. Four modules, shown with different colors, are displayed based on bioinformatics analysis.

Relative expression levels of SPOP, DAXX, RARRES1, and LAMP2

By the $2^{-\Delta\Delta Ct}$ method a statistically significant decrease in SPOP mRNA expression level of malignant prostate tissues was observed in both normal adjacent and BPH tissues (both at $P < 0.001$). As well as, DAXX expression level in PCa tissues was significantly up-regulated in

comparison with both controls (both at $P < 0.001$). The expression of *RARRES1* gene was significantly down-regulated in PCa group in comparison to groups of normal adjacent and BPH samples ($P < 0.001$, $P < 0.011$, respectively). Finally expression of *LAMP2* in PCa samples showed a total significant decreased level compared with normal adjacent and BPH groups (both at $P < 0.001$).

Correlation analysis

The assessment of correlations between expression levels of our four candidate genes in PCa tissues was accomplished (**Table 3**). In this regards, there were significant correlations between *DAXX* and expression levels of *RARRES1* ($r = 0.320$, $P = 0.003$), *LAMP2* ($r = 0.001$, $P = 0.338$), and *SPOP* ($r = 0.220$, $P = 0.029$). The expression of *RARRES1* demonstrated significant correlations with *LAMP2* ($r = 0.373$, $P < 0.0001$) and *SPOP* ($r = 0.351$, $P = 0.001$). In addition, the correlation of *LAMP2* and *SPOP* ($r = 0.535$, $P < 0.0001$) statistically significant.

Table 3. The correlations between expression levels of candidate genes in PCa tissues.

The analysis of correlations between gene expression levels and clinicopathological characteristics such as age, PSA, GS, and Stage of disease in PCa tissues was carried out. *LAMP2* expression was significantly correlated with PSA ($r = -0.31$, $P = 0.05$). However, the other correlation related to four candidate genes did not reach a significance level (**Table 4**).

Table 4. The correlations between gene expression levels and clinicopathological characteristics

ROC curve analysis

The predictive value of gene expressions for discriminating between malignant and non-malignant tissues was investigated by constructing an ROC curve (**Figure 2**). Critical cut-off values of significantly different *RARRES1*, *LAMP2*, *SPOP*, and *DAXX* levels were determined. The area under the curve (AUC), sensitivity, and specificity for *RARRES1* were 0.659, 72.1%, and 53.5%, respectively. AUC for *LAMP2* expression showed the most predictive power, 0.884 (with sensitivity of 90.7% and specificity of 62.8%). As well, the AUC for expression levels of *SPOP* (sensitivity of 86.0% and specificity of 60.5%) and *DAXX* (sensitivity of 86.0% and specificity of 60.5%) as predictors of malignancy in prostate tissue was 0.809 and 0.837, respectively (**Table 5**).

Figure 2. Receiver operating characteristic (ROC) curve showing the area under the curves (AUC) for discriminating between malignant and non-malignant prostate tissues by *DAXX*, *RARRES1*, *LAMP2*, and *SPOP* genes.

Discussion

Gene-module level analysis has emerged as a novel design principle in biological systems. This type of evaluations aims to explain biological network design and system behavior in development of diseases, via highlighting the modules of genes instead of individual genes^(30,31). In the current study, first we enriched the candidate genes and directed biological pathways, by bioinformatics approaches, and their gene network as well as interactions with other genes was designed. Then, expression analysis of *SPOP*, *DAXX*, *RARRES1*, and *LAMP2* was assessed by qRT-PCR in 50 PCa tissues, compared with 50 BPH and 50 normal adjacent prostatic tissues.

Puto et al. described *DAXX* as a transcription factor that serves its suppressive role by recruiting DNA methyl transferases and histone deacetylases in PCa cell lines⁽¹⁶⁾. Here, by developing a network we depicted that *DAXX* mediates its key role in cellular process by interactions with *SPOP* and other factors in pathways related to lysosome, *RARs-mediated signaling*, *PI3K* signaling, and AR activity. *SPOP* encodes an E3 ubiquitin ligase component acting through degradation of several regulators of cell proliferation and apoptosis including *DAXX* in a cancer context⁽³²⁾. Our findings confirms these concepts by showing the inverse relationship between expression levels of *DAXX* (up-regulated) and *SPOP* (down-regulated) and further points to their connection and vital roles as autophagy-related genes in PCa. These results are consistent with those of Ju et al. speculating that *SPOP* selectively suppresses the PCa through stability regulation of cyclin E1 in PCa cell lines. Substantially, expression of cyclin E1 rescues the tumor formation, proliferation, and migration of PCa cells⁽³³⁾. The results from exome sequencing of 112 PCa and normal tissue pairs revealed that *SPOP* gene had the most frequently recurrent mutations influencing its expression level⁽³⁴⁾. Noticeably, Dysregulated levels of *SPOP* may accordingly serve as a specific hallmark in early detection of PCa carcinogenesis⁽³⁵⁾, which can bring us to precise understanding of molecular mechanism and its clinical applications for targeted PCa therapies⁽³⁶⁾. Evidence also suggests that strong expression of *DAXX* correlates with high GS and elevated cell proliferation index, exhibiting its potential prognosticator role in PCa outcomes⁽³⁷⁾.

By considering the network enrichment and correlation outcomes, our study represents for the first the interactions of *RARRES1* and *LAMP2* between themselves and in network of *SPOP* and *DAXX* genes, altogether emphasizing a network developed from different modules (**Figure 1**). Literature introduces *RARRES1* as a putative tumor suppressor gene that negatively regulates the cell proliferation, while less is known about responsible mechanisms ⁽³⁸⁾. Particularly, it has been emphasized that *RARRES1* is involved in autophagy induction ⁽¹⁾. Our network enrichment and qRT-PCR findings supported this hypothesis by revealing the significant reduction of *RARRES1* in tumor samples relative to both controls including adjacent and BPH tissues. Based on the obtained gene network, this reduced level might be indirectly related to the increased levels of *DAXX*, offering their inverse relationship in PCa in our study.

We found a total reduction in *LAMP2* expression level in tumor tissues. Evidence exist that this decreased level can trigger lysosomal membrane permeabilization and subsequently sensitize cells to the lysosomal pathway of cell death ⁽³⁹⁾. Noteworthy, we found that *inosine monophosphate dehydrogenase 1 (IMPDH1)*, as a mediator, interacts with *LAMP2* in autophagy module of our network. This suggests that *DAXX* may be able to down-regulate the *LAMP2* expression through *IMPDH1* in the depicted gene network. On the other hand, *DAXX* can adjust the expression of autophagy-related genes such as *RARRES1* and *LAMP2* by interactions with AR and retinoic acid receptor alpha (*RARA*) (**Figure 1**).

Importantly, the ROC curve analysis showed the good predictive value (AUC above 0.8) for *DAXX*, *SPOP*, and *LAMP2* gene expressions in discrimination of malignant and non-malignant tissues in PCa, among which *LAMP2* had the most sensitivity and specificity. Again, the integrated picture of ROC curve for all four candidate genes, in addition to the significant correlations observed between their expression levels, potentially suggests the putative clinical application of this network.

Conclusion

In conclusion, given the importance of autophagy in PCa tumorigenesis, these findings not only indicate the complicated cellular networks and context-dependent manner of autophagy induction, also suggest that the contribution of *SPOP*, *DAXX*, *RARRES1*, and *LAMP2* together could be a putative regulatory element acting as a prognostic signature and therapeutic target in PCa.

Limitation and Recommendation

In this kind of study, which different molecular techniques can yield different results, it is recommended to study greater sample size with the same methods to increase the accuracy of the results.

As the next step forward, we suggest the study of a more extended gene network from each module to enrich our knowledge of reciprocal interactions between these genes. In line, investigation of their expression alterations in protein level, as well as considering a larger sample size of PCa and BPH tissues, could be of great value for future.

Acknowledgment

We would like to thank all staff of Urology and Pathology department staff in Shohada-e-Tajrish hospital. We would like to show our appreciation towards Dr. Naser Rakhshani and Dr. Arman Morakabatif, for their invaluable help throughout this study.

Conflict of interest

None.

Funding source

Nil.

Author contribution

All authors contributed to the project development and Data collection; Dr. Ranjbar, Dr. Fallah-karkan and Dr. Ghaderian contributed to the Data analysis and Manuscript writing; all authors contributed to the Manuscript editing.

References

1. Roy A, Ramalinga M, Kim OJ, et al. Multiple roles of RARRES1 in prostate cancer: Autophagy induction and angiogenesis inhibition. *PloS one*. 2017;12:e0180344.
2. Taeb J, Asgari M, Abolhasani M, Farajollahi MM, Madjd Z. Expression of prostate stem cell antigen (PSCA) in prostate cancer: a tissue microarray study of Iranian patients. [Pathol Res Pract](#). 2014;210:18-23.

3. Abedi A-r, Fallah-Karkan M, Allameh F, Ranjbar A, Shadmehr A. Incidental prostate cancer: a 10-year review of a tertiary center, Tehran, Iran. *Res Rep Urol*. 2018;10:1-6.
4. Javanmard B, Yousefi M, Yaghoobi M, et al. Ureteral Reimplantation or Percutaneous Nephrostomy: Which One Is Better in Management of Complete Ureteral Obstruction Due to Advanced Prostate Cancer?. *Int J Cancer Manag*. 2017;10: e6074. doi: 10.5812/ijcm.6074.
5. Karkan MF, Razzaghi MR, Javanmard B, Tayyebiazar A, Ghiasy S, Montazeri S. Holmium: YAG Laser Incision of Bladder Neck Contracture Following Radical Retropubic Prostatectomy. *Nephro-Urol Mon*. Online ahead of Print ; In Press(In Press):e88677. doi: 10.5812/numonthly.88677.
6. Quinn DI, Henshall SM, Haynes A-M, et al. Prognostic significance of pathologic features in localized prostate cancer treated with radical prostatectomy: implications for staging systems and predictive models. *J Clin Oncol*. 2001;19:3692-3705.
7. Ghiasy S, Abedi AR, Moradi A, et al. Is active surveillance an appropriate approach to manage prostate cancer patients with Gleason Score 3+ 3 who met the criteria for active surveillance? *Turk J Urol*. 2018:1-4. DOI: 10.5152/tud.2018.72920.
8. Katz B, Reis ST, Viana NI, et al. Comprehensive study of gene and microRNA expression related to epithelial-mesenchymal transition in prostate cancer. *PloS one*. 2014;9:e113700.
9. Saffari M, Ghaderian SMH, Omrani MD, Afsharpad M, Shankaie K, Samadaian N. The Association of miR-let 7b and miR-548 with PTEN in Prostate Cancer. *Urol J*. 2018; 8. doi: 10.22037/uj.v0i0.4564. [Epub ahead of print]
10. Vaezjalali M, Azimi H, Hosseini SM, Taghavi A, Goudarzi H. Different Strains of BK Polyomavirus: VP1 Sequences in a Group of Iranian Prostate Cancer Patients. *Urol j*. 2018;15:44-8. doi: 10.22037/uj.v0i0.3833.
11. Nodouzi V, Nowroozi M, Hashemi M, Javadi G, Mahdian R. Concurrent down-regulation of PTEN and NKX3. 1 expression in Iranian patients with prostate cancer. *International braz j urol*. 2015;41:898-905.
12. Taheri M, Noroozi R, Rakhshan A, Ghanbari M, Omrani MD, Ghafouri-Fard S. IL-6 Genomic Variants and Risk of Prostate Cancer. *Urol J*. 2018; 21. doi: 10.22037/uj.v0i0.4543. [Epub ahead of print]
13. Wisniewski T, Zyromska A, Makarewicz R, Zekanowska E. Osteopontin And Angiogenic Factors As New Biomarkers Of Prostate Cancer. *Urol J*. 2018; 1. doi: 10.22037/uj.v0i0.4282. [Epub ahead of print]
14. Mishra P, Dauphinee AN, Ward C, Sarkar S, Gunawardena AH, Manjithaya R. Discovery of pan autophagy inhibitors through a high-throughput screen highlights macroautophagy as an evolutionarily conserved process across 3 eukaryotic kingdoms. *Autophagy*. 2017;13:1556-72.
15. Draz H, Goldberg A, Sanderson T, Safe S. Diindolylmethane and its halogenated analogues induce autophagy in human prostate cancer cells via induction of the astrocyte-elevated gene-1 (AEG-1). [abstract]. In: *Proceedings of the American Association for Cancer Research Annual Meeting 2017; 2017 Apr 1-5; Washington, DC. Philadelphia (PA): AACR; Cancer Res 2017;77(13 Suppl):Abstract nr 3298. doi:10.1158/1538-7445.AM2017-3298*
16. Puto LA, Benner C, Hunter T. The DAXX co-repressor is directly recruited to active regulatory elements genome-wide to regulate autophagy programs in a model of human prostate cancer. *Oncoscience*. 2015;2: 362–72.
17. Blattner M, Liu D, Robinson BD, et al. SPOP mutation drives prostate tumorigenesis in vivo through coordinate regulation of PI3K/mTOR and AR signaling. *Cancer cell*. 2017;31(3):436-451.
18. Mani R-S. The emerging role of speckle-type POZ protein (SPOP) in cancer development. [Drug Discov Today](#). 2014;19:1498-1502.
19. Puto LA, Reed JC. Daxx represses RelB target promoters via DNA methyltransferase recruitment and DNA hypermethylation. [Genes Dev](#). 2008;22:998-1010.
20. Tang HW, Wang YB, Wang SL, Wu MH, Lin SY, Chen GC. Atg1-mediated myosin II activation regulates autophagosome formation during starvation-induced autophagy. *The EMBO journal*. 2011;30:636-51.

21. Zalckvar E, Berissi H, Eisenstein M, Kimchi A. Phosphorylation of Beclin 1 by DAP-kinase promotes autophagy by weakening its interactions with Bcl-2 and Bcl-XL. *Autophagy*. 2009;5:720-22.
22. Taheri M, Noroozi R, Dehghan A, et al. Association study of Retinoic Acid Related Orphan Receptor A (RORA) gene and risk of prostate disorders. *Urol J*. 2018; 22. doi: 10.22037/uj.v0i0.4373. [Epub ahead of print]
23. Anguiano J, Garner TP, Mahalingam M, Das BC, Gavathiotis E, Cuervo AM. Chemical modulation of chaperone-mediated autophagy by retinoic acid derivatives. *Nat Chem Biol*. 2013;9:374-82.
24. Morell C, Bort A, Vara-Ciruelos D, et al. Up-regulated expression of LAMP2 and autophagy activity during neuroendocrine differentiation of prostate cancer LNCaP cells. *PloS one*. 2016;11:e0162977.
25. Epstein JI, Egevad L, Amin MB, Delahunt B, Srigley JR, Humphrey PA. The 2014 International Society of Urological Pathology (ISUP) consensus conference on Gleason grading of prostatic carcinoma. *Am J Surg Pathol*. 2016;40:244-52.
26. Kutmon M, Kelder T, Mandaviya P, Evelo CT, Coort SL. CyTargetLinker: a cytoscape app to integrate regulatory interactions in network analysis. *PloS one*. 2013;8:e82160.
27. Carlin DE, Demchak B, Pratt D, Sage E, Ideker T. Network propagation in the cytoscape cyberinfrastructure. [PLoS Comput Biol](#). 2017;13:e1005598.
28. Türei D, Földvári-Nagy L, Fazekas D, et al. Autophagy Regulatory Network—A systems-level bioinformatics resource for studying the mechanism and regulation of autophagy. *Autophagy*. 2015;11:155-65.
29. Agell L, Hernández S, Nonell L, et al. A 12-gene expression signature is associated with aggressive histological in prostate cancer: SEC14L1 and TCEB1 genes are potential markers of progression. *Am J Pathol*. 2012;181:1585-94.
30. Wang X, Dalkic E, Wu M, Chan C. Gene module level analysis: identification to networks and dynamics. *Curr Opin Biotechnol*. 2008;19:482-91.
31. Razzaghi MR, Mazloomfard MM, Malekian S, Razzaghi Z. Association of macrophage inhibitory factor-173 gene polymorphism with biological behavior of prostate cancer. *Urol J*. 2018 Aug 14. doi: 10.22037/uj.v0i0.3968. [Epub ahead of print]
32. Puto LA, Brognard J, Hunter T. Transcriptional repressor DAXX promotes prostate cancer tumorigenicity via suppression of autophagy. *Journal of Biological Chemistry*. 2015;jbc. M115. 658765.
33. Ju L-G, Zhu Y, Long Q-Y, et al. SPOP suppresses prostate cancer through regulation of CYCLIN E1 stability. [Cell Death Differ](#). 2018;1. oi.org/10.1038/s41418-018-0198-0.
34. Barbieri CE, Baca SC, Lawrence MS, et al. Exome sequencing identifies recurrent SPOP, FOXA1 and MED12 mutations in prostate cancer. *Nat Genet*. 2012;44:685.
35. Wang H, Barbieri CE, He J, et al. Quantification of mutant SPOP proteins in prostate cancer using mass spectrometry-based targeted proteomics. *J Transl Med*. 2017;15:175.
36. Boutros PC. The path to routine use of genomic biomarkers in the cancer clinic. *Genome Res*. 2015;25:1508-13.
37. Tsourlakis MC, Schoop M, Plass C, et al. Overexpression of the chromatin remodeler death-domain-associated protein in prostate cancer is an independent predictor of early prostate-specific antigen recurrence. *Hum Pathol*. 2013;44:1789-96.
38. Rivera-Gonzalez GC, Droop AP, Rippon HJ, et al. Retinoic acid and androgen receptors combine to achieve tissue specific control of human prostatic transglutaminase expression: a novel regulatory network with broader significance. *Nucleic Acids Res*. 2012;40:4825-40.
39. Fehrenbacher N, Bastholm L, Kirkegaard-Sørensen T, et al. Sensitization to the lysosomal cell death pathway by oncogene-induced down-regulation of lysosome-associated membrane proteins 1 and 2. *Cancer Res*. 2008;68:6623-33.

Corresponding Authors

Seyyed Mohammad Hossein Ghaderian, E-mail address: sghaderian@sbmu.ac.ir

Department of Medical Genetics, Shahid Beheshti University of Medical Sciences. Velenjak Blvd.

Kodakyar Close, Tehran, IRAN. Post Code: 1985717443; Tele Fax: + 98 21 23872572

Tables and Figures Legends

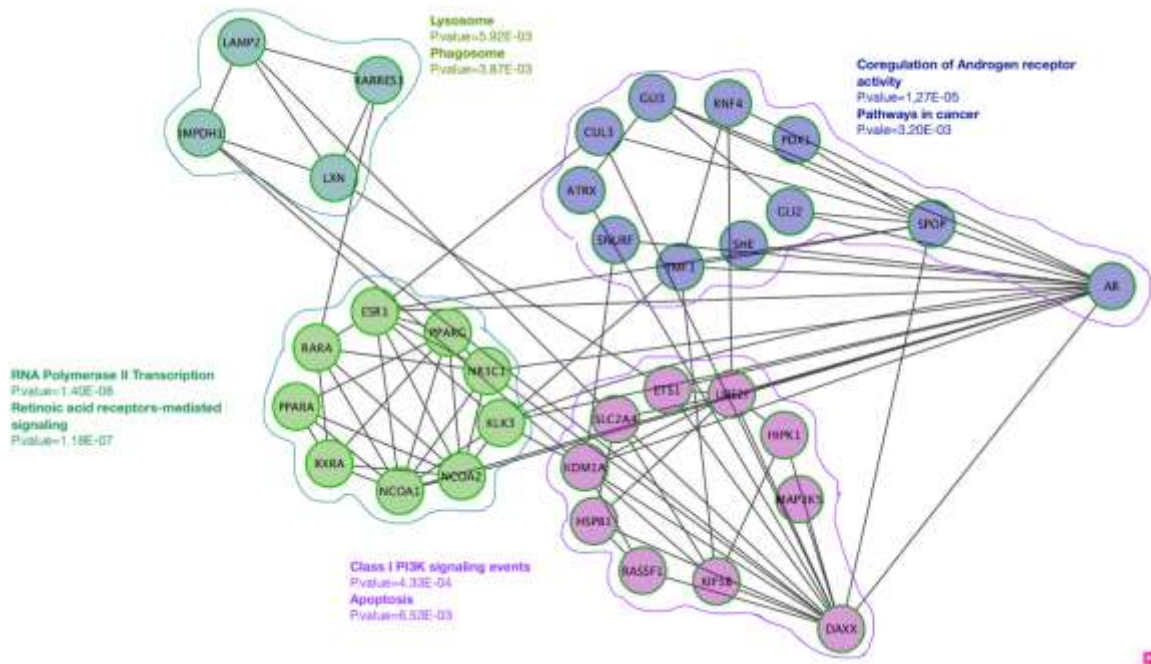


Figure 1. Four network clustering modules based on bioinformatics analysis, shown with different colors.

Table 1. The sequences of primers used in this study.

Gene	Primer sequences	Primer length	Product length
B2M	F: AGATGAGTATGCCTGCCGTG	20	105
	R: GCGGCATCTTCAAACCTCCA	20	
RARRES1	F:	22	110
	CTAGTGTGAGGCAGTGGAAAAC		
	R: GACCAAGTGAATGCGACAGG	20	
LAMP2	F: ATGGCTCCGTTTTTCAGCATTG	21	106
	R: GCTCCAGACACTGAAACAGTC	21	
SPOP	F: TACCCTCTTCTGCGAGGTGA	20	129
	R: CGGGAATTCTCCCACAGTCC	20	
DAXX	F: GACTATAGGCCAGGCGTTGA	20	144
	R: CTCGCCCTCCTCACTTTTGT	20	

Table 2. The association of four candidate genes with clinicopathological characteristics of PCa patients.

Table 3. The correlations between expression levels of candidate genes in PCa tissues.

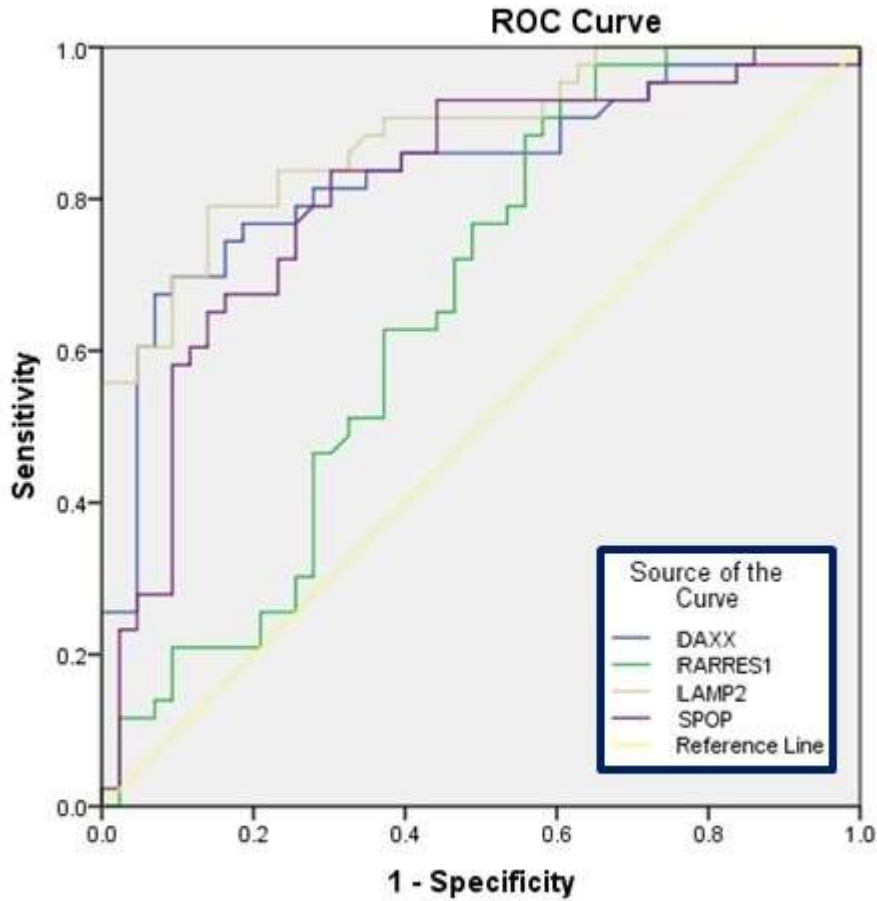
Correlations		DAXX	RARRES1	LAMP2	SPOP
DAXX	Correlation Coefficient (r)	1.000	0.320	0.338	0.220
	Sig. (2-tailed)	.	0.003 **	0.001 **	0.029 *
RARRES1	Correlation Coefficient (r)		1.000	0.373	0.351
	Sig. (2-tailed)		.	>0.0001 **	0.001 **
LAMP2	Correlation Coefficient (r)			1.000	0.535
	Sig. (2-tailed)			.	>0.0001 **
SPOP	Correlation Coefficient (r)				1.000
	Sig. (2-tailed)				.

* Correlation is significant at the 0.05 level (2-tailed).

** Correlation is significant at the 0.01 level (2-tailed).

Table 4. The correlations between gene expression levels and clinicopathological characteristics

Gene	Age		PSA		GS		Stage	
	<i>R</i>	<i>P-value</i>	<i>R</i>	<i>P-value</i>	<i>R</i>	<i>P-value</i>	<i>R</i>	<i>P-value</i>
DAXX	-0.18	0.22	0.033	0.84	-0.14	0.36	-0.026	0.86
RARRES1	-0.07	0.61	0.17	0.3	-0.08	0.57	-0.12	0.42
LAMP2	0.22	0.14	-0.31	0.05	-0.07	0.61	-0.14	0.37
SPOP	0.25	0.09	-0.23	0.14	-0.01	0.92	-0.13	0.38



Diagonal segments are produced by ties.

Figure 2. Receiver operating characteristic (ROC) curve showing the area under the curves for discriminating between malignant, BPH tissues by DAXX, RARRES1, LAMP2, and SPOP genes.

Table 5. The results obtained from ROC curve analysis of four candidate genes.

Gene	Cut-off point	AUC	95% Confidence Interval	%Sensitivity	%Specificity	<i>P-value</i>
DAXX	-6.302	0.837	[0.751-0.924]	86	60.5	<0.0001
RARRES1	-2.557	0.659	[0.542-0.776]	72	53.5	0.011
LAMP2	-3.065	0.884	[0.815-0.953]	90.7	62.8	<0.0001
SPOP	-2.437	0.809	[0.715-0.904]	86	60.5	<0.0001